IEEE Access
Multidisciplinary ⋮ Rapid Review ⋮ Open Access Journal

Received October 22, 2020, accepted November 1, 2020, date of publication November 5, 2020, date of current version November 18, 2020.

Digital Object Identifier 10.1109/ACCESS.2020.3036134

Effective Hybrid Method for the Detection and Rejection of Electrooculogram (EOG) and Power Line Noise Artefacts From Electroencephalogram (EEG) Mixtures

MOHAMMED ALI AHMED[1], DEYU QI[1], AND EBTESAM N. ALSHEMMARY[2,3]

[1]College of Computer Software, South China University of Technology, Guangzhou 510640, China
[2]IT Research and Development Centre, University of Kufa, Najaf 54001, Iraq
[3]Biomedical Engineering School, Southern Medical University, Guangzhou 510515, China

Corresponding author: Mohammed Ali Ahmed (mod326432@yahoo.com)

ABSTRACT Electrooculogram (EOG) and power line noise artefact detection and rejection have commonly utilized Stone's blind source separation (Stone's BSS) algorithm. The paper suggests a hybrid method between particle swarm optimization (PSO) and Stone's BSS for the detection and rejection of electrooculogram (EOG) and power line noise in the single-channel without the use of a notch filter. The proposed method contains three major steps: centralizing and whitening of the input EEG signal, incorporating the processing EEG signal into the iterative algorithm of the particle swarm optimization (PSO) to randomly generate the optimal value of (h_{short}, h_{long}) and weight vector W parameters, and applying Stone's BSS using the generalized eigenvalue decomposition (GEVD) method to eliminate electrooculogram (EOG) and power line noise artefacts to obtain a clean EEG signal. The authors assess the robustness of the suggested method evaluated using real and simulated electroencephalogram (EEG) data sets. The simulated electroencephalogram (EEG) data and electrooculogram (EOG) and line noise (LN) artefacts are produced and mixed randomly in the MATLAB program; two types of real EEG data are taken in 9 and 19 channels. Evaluation results show the proposed algorithms as effective techniques for extracting both the power line noise and electrooculogram (EOG) artefacts from brain mixtures compared to specific BSS algorithms (e.g., Stone's BSS, evolutionary fast independent component analysis (EFICA), fast independent component analysis (FastICA), and joint approximate diagonalization of Eigen matrices (JADE)) while preserving the clinical features of the reconstructed EEG signal.

INDEX TERMS Electroencephalogram (EEG), electrooculogram (EOG), particle swarm optimization, signal analysis, Stone's BSS technique.

I. INTRODUCTION

Electroencephalography is a technique used in biomedical signal processing studies to describe the human brain's behaviour. Electroencephalogram (EEG) signals are generated by cortical neuron-correlated reciprocal behaviour. Brain efficiency is measured with sense nodes linked to the head of the patient [1]. The first paper that portrayed the method for the recognition of human brain output was written in 1929. The essential features of the EEG signals are demonstrated without difficulty by the multiple sensors (electrodes), the spatial and temporal reference set, perfect for the dependence on electrode magnitude and time-based applications [2]. EEG signals comprise a mixed signal of unintentional effects during the measurement cycle, such as electrooculogram (EOG) and control system disruptions, making it hard for EEG brain function to study. EEG signals in the 0–16 Hz frequency band in microvolts, with a 0–64 Hz frequency range, are affected by electrooculogram (EOG). Such an undesirable blend should be removed from the EEG. Electrooculogram (EOG) is the out-of-control activity of the eye that parasitizes the requisite brain-signal effects for the functionality of the brain-computer interface [3].

Researchers have advanced sundry techniques over the years to efficiently remove the artefact and noise. One of the most commonly used methods to extract artefacts is the use of

The associate editor coordinating the review of this manuscript and approving it for publication was Vivek Kumar Sehgal.

dependent variable variation, named independent component analysis (ICA), where the original signals are decomposed in a brand-new linear combination signal called independent parts (ICs). ICA helps to classify the artefacts in the provided brain signal. In comparison, Corradino *et al.* [4] suggested a system that allows using regression ICA. The method can avoid the loss of information by using a feedback control system to test the consistency and recognize the artefacts residual that reflect artefacts significantly. Subsequently, computational regression used to measure the association's coefficient between the recognized ICs artefacts and the original signal to confirm the artefact components deletion correctly without informational loss. The method was efficient, as it has been shown that the purified ICs relate to a comparable data signal in all bands. Applying ICA algorithms often causes a problem of distortion of the raw EEG signal. To overthrow this difficulty, Gauba *et al.* [5] have implemented an average moving (MA) filter to enhance the signal by merely replacing each data value by the average adjacent ICA values. The original signal is smoothed after application of the MA filter. It calculates the moving average by using the model:

$$\overline{y}[i] = \frac{1}{M} \sum_{j=0}^{M-1} x[i+j] \tag{1}$$

where $\overline{y}$[i] is the output signal, x is the received signal, and M is the point's number utilized during the average computation.

To simultaneously extract muscle and ocular artefacts, Chen *et al.* [6] introduced an expanded variant of ICA from one or more datasets. It utilizes information theory principles to divide each set of data into mutually independent sources, while also using a dependency association between sets of data to rely on similar sources across data sets. The suggested approach employs simultaneous independent vector analysis (IVA) for jointly used higher-order statistics (HOS) and second-order statistics (SOS). IVA makes use of HOS in combination with SOS ensuring source statistical independence. Whereas the different data sets are multichannel records time delayed, IVA uses SOS to search the information of potential sources' temporal structure. IVA incorporates the strengths of both HOS and SOS, that separate the EEG's ocular and muscle objects. Their analysis was performed with simulated data and actual EEG data. The findings both show that their approach has a successful signal and noise ratio (SNR).

In addition to the above methods, several researchers have introduced wavelet transformation to distinguish artefacts from EEG signals. However, the general way to remove artefacts using wavelet transform may cause data loss, and clean signals may be reconstructed incorrectly. Much work is done that incorporates the wavelet transformation with other approaches for further developing the general process. Mammone *et al.* [7] suggested a system famed as automatic wavelet independent component analysis (AWICA) for a multichannel scalp EEG rejection of automated artefacts.

The EEG input is decomposed through the discrete wavelet transforms (DWT) into four major brain function strips to partition each initial data collection channel. A wavelet component (WC) represents every rhythm of each channel. To concentrate the artefacts into a few ICs, the ICA analytics will be channelled to each WCs. It automatically detects and eliminates the resulting artefactual wavelet independent components (WICs). The clean signal reconstruction subsequently includes two steps, which are the inverse ICA and the inverse DWT. Study of Szibbo *et al.* [8], Addresses a simple blink filtering system with a smoothing filter of Savitzky-Golay (SG) and contrasts it with Independent Component Analysis, an agreed blink removal system. The SG-based blink filtering method arose from the need for blink removal in EEG systems with a low number of channels and low processing capacity, specifically reading from the front position where the blink disruption is significant, however, several disadvantages to the SG-based approach, for example, difficult to detect blinking components from channels situated further from the forehead, and also the claim that the retraction of EOG operation in the time or frequency domain necessarily requires the subtraction of a part of the EEG concerned. In [9], the author proposes a system for classifying event-related potentials to improve accurate classification and efficiency depends on the required range of classifier parameters and features from dense-array electroencephalography (EEG) signals. Using a combination of a Fisher Discriminant Analysis (FDA) and a multi-objective hybrid real-binary Particle Swarm Optimisation (MHPSO) algorithm, the proposed approach has achieved higher classification accuracy than that achieved by conventional approaches. Research in [10] using particle swarm optimization (PSO) to remove ECG artefact from simulated and real Electroencephalogram (EEG) data sets, by tuning the parameters of adaptive neuro-fuzzy inference system (ANFIS) individually, The performance of the techniques is higher than the current traditional approaches.

Kaur and Singh [11], implemented a second-order blind identifier (SOBI) based ICA using wavelet thresholding in their work. Artefact based ICs were detected using SOBI ICA, followed by thresholding for wavelets. Wavelet thresholding is applied based on soft thresholding to DWT's recovered coefficients to distinguish the artefact ICs from any other operation. The parameters of root mean square error (RMSE) and peak signal-to-noise ratio (PSNR) is calculated for assessing the efficiency of the proposed system. It indicates that their behaviour renders artefacts better concealed.

Many of the previous research utilized ICA, that have several drawbacks: an output components' equal number and results, source distortion, output component abnormalities, and the amplitude information's lack in the output components.

The Stone BSS among the source separation methods, that with no details on the source signals or the mixed matrix, it can distinguish the source signals from the mixed signals. Abdullah and Zhu [12] proposed a modification of Stone's BSS based on the Fast Genetic Algorithm (FGA), and hybridization was used to generate and modify the optimal half-life (h_L, h_S) parameters that affect the stone system

separation mechanism by using the reactions of two separate linear scalar filters for the same set of signals. Fast genetic algorithms are an effective method to improve the process of segregation when hybridised with SBSS algorithms. This hybridisation is for the purification of EEG brain signals from multiple artefact forms. In this study, present a new application for Stone's Blind Source Separation method in brain signal analysis to separate an EOG and power line noise artefacts from electroencephalogram (EEG) mixtures with PSO hybridization to enhance the separation process. We consider the algorithm suggested by the authors M. A. Ahmed, *et al.* in [13] to evaluate the efficiency of the suggested method. The evolution of the method is based on the rejection of other artefacts, such as electrooculogram (EOG) and power line noise artefacts from the EEG mixture. The real and simulated EEG used in this evolution; the real EEG database contains 9 channels and 19 channels, and simulated EEG data and artefacts were implemented using MATLAB software 2018. Two methods used to assess the separation process in the real EEG database are the sparsity measure and the correlation between the artefact-reference signal; in simulated data, an integral square error (ISE) and carrier-to-interference ratio (CIR) are used to measure the separation process. The contributions of this work validate the reliability and robustness for electrooculogram (EOG) and power line noise artefact removal by the suggested algorithm in [10].

Therefore, further evolution of the suggested algorithm is possible by applying the algorithm to clean EEG with other artefacts such as electrocardiography (ECG) signals. Other ways to improve the process of separation by hybridizing the suggested system with soft computing techniques, such as artificial bee colony algorithms (BCA) and the runner-root algorithm (RRA).

The rest of this paper is organized as follows. Section II presents the EEG database related to this work. Section III presents a brief overview related to the suggested method with a focus on the main process and equations that work in conjunction between Stone BSS and PSO algorithms. This is followed by section IV, which contains the results and discussion, wherein the validation scheme for evaluating the separation process is discussed, and the synthesis of EEG artefacts and the experiment results are presented in this section. The conclusion is drawn in section V.

II. PROPOSED WORK DATA SET

The EEG utilizes scalp-mounted sensors to transmit electrical signals through the cortex. The sensors are placed using an international 10-20 strategy. Two data sets are utilized in this study, virtual (simulated) EEG data by MATLAB R2018, and real EEG data.

A. REAL EEG DATA

The brain computerized interface (BCI) system is utilized to calculate patients' EEG signals. The system has nine-channel sensors and 0-256 Hz sampling frequency [14]. Two forms of real EEG data are registered on 9 and 19 channels; for 9-channel data, EEG signals are polluted with EOG and 50-Hz power line noise. The 19-channel data collection is polluted with power line noises and EOG error registered by computerized EEG devices at Al-Jomhori hospital, Taiz, Yemen.

1) NINE-CHANNEL DATA SET

The BCI system's obtained data was sampled at 256 Hz with 2 minutes maximum length. The ISR tests the efficiency of the algorithm by using simulated data but doesn't accept to the actual EEG data because of the unknown combining mechanism. Then correlation analysis utilized to assess the removal process of the suggested methods. Nine channels have been utilized in this work, in which six sensors (Fp1, Fp2, C3, C4, O1, and O2) are utilized according to the (10-20 method) to measure the brain signals located on the scalp: one sensor positioned at Cz (Figure 1) as a ground, and two EOG sensors (vEOG and hEOG) mounted above and on the left eye socket to start measuring EOG activity from the eyes and the face.

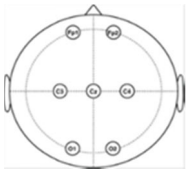

FIGURE 1. The electrodes place.

Recording EEG signals are tainted with EOG artefacts and (50 Hz) power line noise. The EOG artefact is present in the frontal channels and frontopolar channels like Fp1, Fp2, F7, and F8 and decreases when the spacing of the sensors from the eye increases. All the EEG data are polluted with 50-Hz power line noise but are heavily contaminated differently. Power line noise is prevalent on the central (C3 & C4) and occipital (O1 & O2) channels, as shown in Figure 2 [15].

2) NINETEEN-CHANNEL DATA SET

Real EEG 19-channel data were distorted by power line noise interference and EOG interference captured by computer-based EEG systems at Al-Jomhori hospital, Taiz, Yemen. Computer-based EEG is a PCI data capture card computer that receives input from the scalp via macro sensors. One normal person, a 32-year-old male, partake in the study. EEG signals captured using 19 electrodes mounted on the scalp according to the 10-20 system used to measure brain signals. Based on the design of the computer-based EEG system, the measured signals are digitized at 256 Hz with a trail duration of 10 sec (10 sec $\times$ 256 Hz $=$ 2560 specimens), in which the participant was enabled to produce EOG artefacts (eye blinking & eye movement).

If the EEG report has been finished, it can be stored as an ASCII code; this ASCII document can be viewed via notepad software. The data are imported into Microsoft Excel

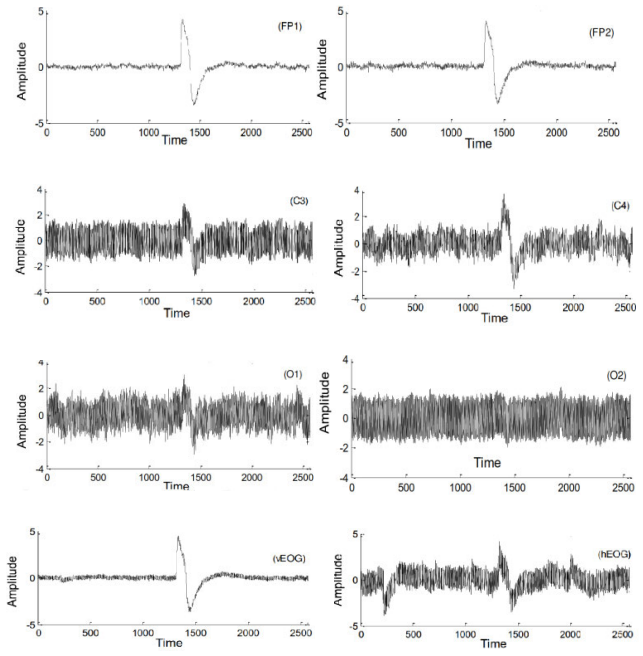

FIGURE 2. Set of data I with zero mean and unit variance.

to delete the first column containing the timing information and removing the channel name, and then data are imported into MATLAB. Figure 3 indicates polluted signals; these signals are pre-processed (centralizing and whitening) for simplification, as seen in Figure 4.

B. SIMULATED EEG DATA SET

In the MATLAB as shown in Figure 5, artificial EEG, EOG and power lines are created. Multiple artefact forms and EEG signal emulation are carried out based on each signal's specification.

According to Abdullah and Zhu [12], the generation of artificial EEG signals is polluted with EOG and power line noise using classical event-related potentials (ERP) theory. The additional signal and noise components produce the simulated data. The two functions: peak and noise can generate two components. The noise function in MATLAB is created in such a way that the power spectrum matching the power spectrum of the human's EEG. In general, the noise function has three parameters: the first to describe the length of a single signal test by the number of samples, the second to describe the number of tests, and the third to describe the sampling frequency [16]. Therefore, for one test generation of 0.8 s of noise with a sampling frequency of 250 Hz, one trial can be typed in MATLAB as Mynoise = noise (200, 1, 250).

The value of the first parameter representing the number of samples was determined by multiplying the noise length by the sampling frequency, i.e., 0.8*250 = 200. The function produces a sample-containing vector. This can now be visualized by typing: plot (Mynoise).

The function peak is somewhat close in form, but it has other parameters, including a 4th and 5th parameters defining the peak frequency and the middle location of the peak,

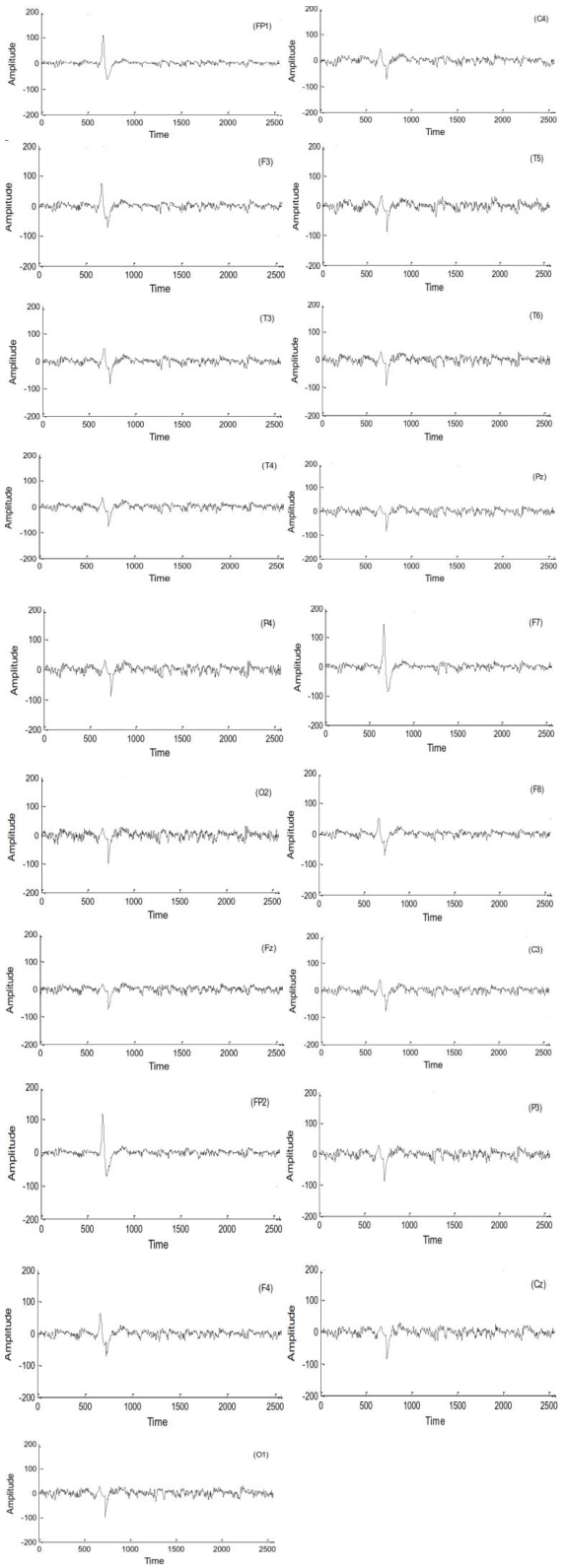

FIGURE 3. The measured signals by a computerized EEG device.

respectively. It can type Mypeak = Peak (200, 1, 250, 5, 115) if, for example, want to produce and show a peak at a frequency of 5 Hz and a centre in the 115th sample.

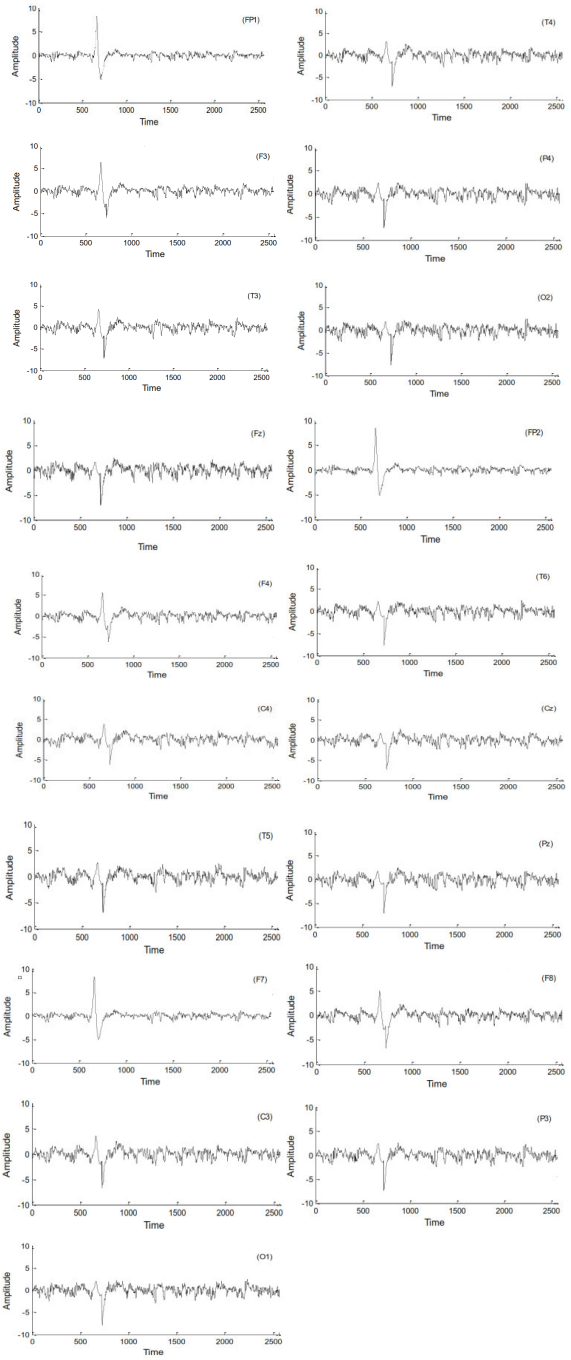

FIGURE 4. Measured signals with the unit (mean and variance).

Once both the signal and noise are created, then they can be combined. If the peak wants to be (−ve), it can be multiplied by −1 before adding, and the amplitudes of the signal and noise can be determined by multiplying the vectors that represent them before adding, such as Mysignal = (−5) ∗ Mypeak + 3 ∗ Mynoise.

To produce multiple trials of signal, the number of trials needs to be defined in the second parameter of the peak and noise of the function. The resulting data structure would be a vector of concatenated signals. When generating multiple

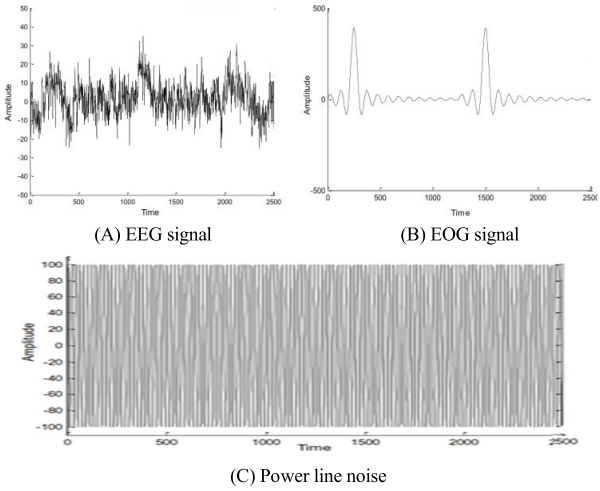

FIGURE 5. The artificial sources.

trials, the 6th parameter can be defined in the function peak that defines the time jitter of the peak during the trials. To produce data from multiple electrodes, you can build a multi-row matrix with the same number of electrodes for each electrode separately and each row can be the same as the signal of an electrode. Furthermore, it should be noted that the peaks in various electrodes have various amplitudes, so the coefficients of the dipole model should be scaled. The pseudo-code for the simulation of EEG data (973 studies and 31 electrodes) is as follows:

Algorithm 1 The Steps to Generate Simulated EEG Signals

Required: MATLAB EEG toolbox.

Output: The resulting data structure is a vector of concatenated signals

Steps:

1. Initialize the general parameters of the EEG signal Frames, Trials, Srate.
2. Initialization Noise parameters Neamp, Nefreo, Nepos.
3. Initialization Peak parameters PeAmp, PeFreq, PePos.
4. Generating multiple trials, and defined it in the function peak that initializes the time jitter of the peak during the trials and amplitude of noise NoiseAmp.
5. Calculate the NE by multiplying the NeAmp with the output from the peak.
6. Calculate the PE by multiplying the PeAmp with the output from the peak.
7. Generate EEG data for every electrode separately and create a multi-row matrix equivalent to the number of electrodes where each row meets a one electrode signal by multiply Ne and Pe with the dipole model and adding the results.
8. Scaled the coefficients of the dipole model to generate peaks with different amplitude in different electrodes.

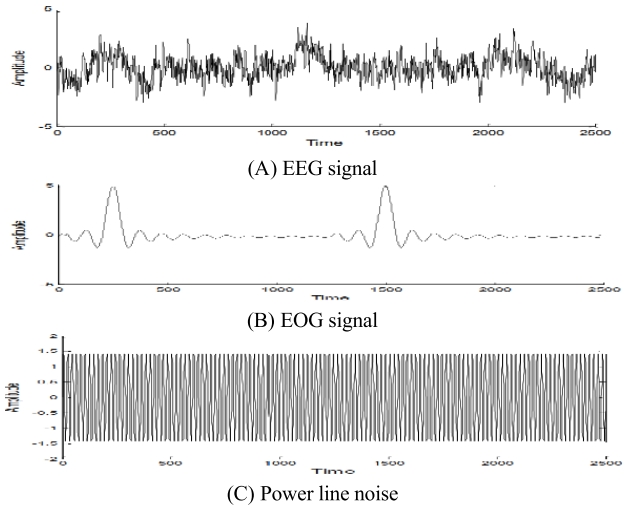

FIGURE 6. The artificial source with the zero mean and unit variance.

EOG is generated through a sine function and is randomly intersected by a combination of signal to build a mixed-signal (Figure 5). Artificial sources are simplified by pre-processing (centralizing and whitening) to obtain sources with zero mean and unit variance, as shown in Figure 6. Signals are randomly combined by adding the "A" matrix to produce the "X" mixture.

The mixing process has all the possibilities are used to contain all the planned mixtures and to generate various mixture styles, as shown in Figure 7 to Figure 9. The artificial EEG signals and power line noise interference (LN) are combined randomly to generate combinations as shown in Figure 7.

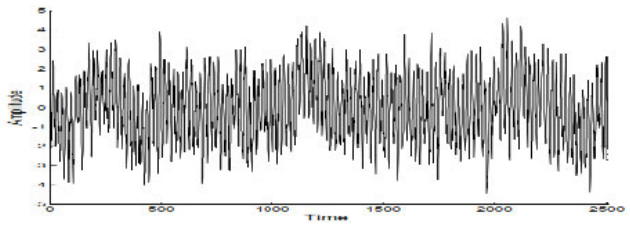

FIGURE 7. Mixture 1 signals (EEG contaminated by LN).

Figure 8 shows the mixing between the simulate EEG signal and electrooculogram (EOG) artefact; the sources are mixed randomly to produce the mixture.

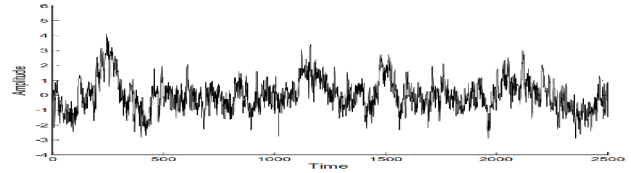

FIGURE 8. The mixture 2 signals (EEG contaminated by EOG).

Figure 9 shows the mixing between the simulated EEG signal with electrooculogram (EOG) and power line noise interference (LN). The random mixing process with the random mixing matrix was used to produce these mixtures.

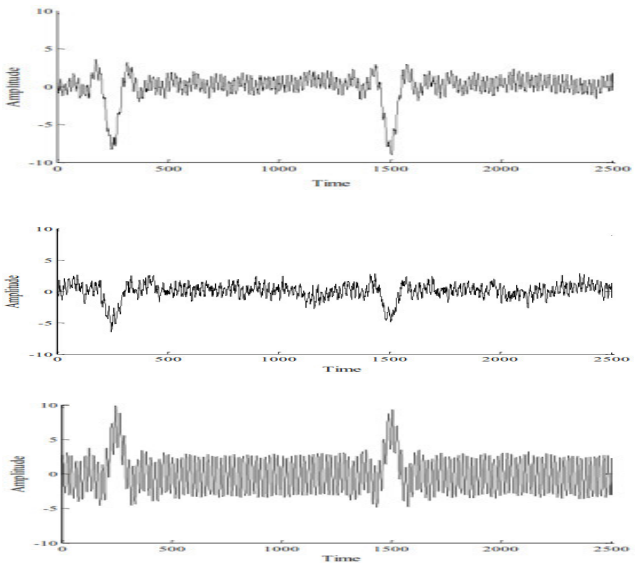

FIGURE 9. Mixture 3 (EEG contaminated by EOG and LN).

III. PROPOSED METHOD

It uses the PSO algorithm for gradual calculation of the optimal half-life value (h_{short}, h_{long}) to perform the segregation method. The value of (h_{short}, h_{long}) is set in the original Stone's BSS, usually ($h_{long} \geq 100h_{short}$). PSO alone has a few drawbacks in the solution of BSS, like the accuracy of the W segregation vector, which is related to the random generation of main parameters, and the sluggish rate of extraction caused by the magnitude increase of the solution space.

In the suggested method, the (h_{short}, h_{long}) value is progressively developed to improve the separation process. The signal mix will be mutually independent when ($h_{short} \rightarrow 0$) and ($h_{long} \rightarrow \infty$) is specified. Stone's blind source separation used to transform the X signal to an isolated independent, that is statistically not fully independent signal. It uses the PSO rather than a fixed value to establish random optimum (h_{short} and h_{long}) parameters and to change these parameters until it has fulfilled the last conditions. The suggested method comprises 2 steps: first, get the initial splitting matrix $W_{Initial}$ using the original Stone's BSS with the random parameters of (h_{short} and h_{long}) that adjusted by the PSO algorithm until we have met the stop requirements.; second, get the optimum split W_{Refine} matrix by harmonized $W_{Initial}$ using the PSO as a refinement process for the coefficients of $W_{Initial}$ to create W_{Refine}as explains in Algorithm 2.

Stone's BSS is used as a temporal predictability measurement (TPM) to distinguish data from the key data, combining, and speculation. For the signal $y(k)$, The following specifies the TPM [17]:

$$F(y) = \log \frac{V_y}{U_y} = \log \frac{\sum_{K=1}^{N} (y_{long}(k) - y(k))^2}{\sum_{k=1}^{N} (y_{short}(k) - y(k))^2} \quad (2)$$

$$y_{short}(k) = \beta_s y_{short}(k-1)(1-\beta_s)\, y(k-1) \quad (3)$$

Algorithm 2 The Major Steps for PSO to Generate Random Parameters and Tune to Stone's BSS

Required: EEG Signals.

Steps:

1. Initialization of the parameters ω, α^1, α^2, n.
2. Generateh_{long}, h_{short} and $W_{Initial}$ randomly.
3. Run the traditional Stone's BSS.
4. Re-arrange and measure the fitness function to assess the expense of the proposed plan (Particle X(i)).
5. Calculate X(i) costs when it is less than l_{best}(i) costs, then proceed to step 6; otherwise, proceed to step 7.
6. Updates local bests (l_{best}(i) = X(i)), updates global bests, and updates velocities and positions.
7. Meet the stopping requirement for a maximum generations number >25 and proceed to step 8; otherwise, proceed to step 3.
8. Obtain the optimal solution of h_{long}, h_{short} and W_{ISBSS}.
9. Gain the EEG signals.
10. End.

$$y_{long}(k) = \beta_L y_{long}(k-1) + (1-\beta_L)\, y(k-1) \tag{4}$$

where the total data for y (k) is N, $\beta_s = 2^{-1/h_{short}}$, $\beta_L = 2^{-1/h_{long}}$, and h_{short}, h_{long} are the variables of half-life. The half-life (h_{short}) of β_s are 100 periods shorter than the half-life (h_{long}) of β_L. These values are determined by Eqs. (5&6) using the suggested method:

$$h_{long\ i+1} = h_{long\ i} + \gamma \tag{5}$$

$$h_{short\ i+1} = h_{short\ i} + \gamma \tag{6}$$

where the random value is γ, the new h_{long} value is $h_{long\ i+1}$, and $h_{short\ i+1}$ is the new h_{short} value. According to Eq.5 and Eq.6, if y(k) = $w_i^T x(k)$, and $W = [w_1, w_2, \ldots - w_n]$, Eq.2 will be rewritten as follows [18]:

$$F(y_i) = log\frac{w_i c_{xx}^{long} w_i^T}{w_i c_{xx}^{short} w_i^T} \tag{7}$$

where C_{xx}^{long} is a long-range covariance array ($N \times N$) among the signal combinations, and $C_{x_i x_j}^{long}$ and $C_{x_i x_j}^{short}$ among the i_{th} and j_{th} blends, respectively, are defined as follows:

$$C_{x_i x_j}^{short} = \sum_t \left(x_{it} - x_{it}^{short}\right)\left(x_{jt} - x_{jt}^{short}\right) \tag{8}$$

$$C_{x_i x_j}^{long} = \sum_t \left(x_{it} - x_{it}^{long}\right)\left(x_{jt} - x_{jt}^{long}\right) \tag{9}$$

Using the Stone method, S from X is retrieved without "A" identification. The collected signals are determined according to the extraction model as follows:

$$Y(k) = WX(k) \tag{10}$$

where $Y(k) = [y_1(k), \ldots, y_n(k)]^T$ is the system or sensing factor blend data (known), $X(k) = [x_1(k), \ldots, x_n(k)]^T$ is the (unknown) source data, T corresponds to the operator for transposition, $W \in R^{(n\times n)}$ is the (unknown) mixture of data and k is an indicator of time. Stone's system starts with the quest for the original $W_{Initial}$ separator matrix. For the ($W_{Initial}$ and W_{Refine}) coefficients' acquisition, it uses the PSO as an optimization tool. As an initial parameter, PSO algorithms use $W_{Initial}$ to render an independent X signal variable with the fitness function.

The fitness function parameter (Fit) definition is the PSO algorithm's key to success. The PSO aims to improve the fitness function by reducing shared information $I(y)$ between the elements. Start the fitness function:

$$Fit(y) = \frac{1}{I(y) + \varepsilon} = \frac{1}{\sum_{i=1}^{n} H(y_i) - H(y_1, y_2, \ldots, y_n)} \tag{11}$$

where $y_1, ..., y_n$ is a separated signal, H is signal entropy, $I(y)$ is the definition of the difference between n signals entropy computed for the shared information, and ε is a constant value (0.0001). The initialisation configurationsof PSO are as follows:

$f : R^m \to$ úR;	fitness function
n = 20 . . . − 200;	particle's number
$x_i \in R^m, i = 1 \ldots - n$;	particle positions
$v_i \in R^m, i = 1 \ldots - n$;	particle velocities
$\hat{x}_i$;	current best of each particle
$\hat{g}$,	global best and $\omega, \alpha_1, \alpha_2$ constants

For each particle $i = 1 \ldots - n$,

- Create random vectors r_1, r_2 with components in $U[0, 1]$;
- Update velocities $v_i \leftarrow \omega v_i + \alpha_1 r_1^{\circ}(\hat{x}_i - x_i) + \alpha_2 r_2^{\circ}(\hat{g} - x_i)$;
- Update positions $x_i \leftarrow x_i + v_i$;
- Update local bests $\hat{x}_i \leftarrow x_i iff\, (x_i) < f(\hat{x}_i)$;
- Update global best $\hat{g} \leftarrow x_i iff\, (x_i) < f(\hat{g})$;
- Initialize the positions of particles and their velocities accordingly:

$$X = lower_{limit} + \left(upper_{limit} - lower_{limit}\right) \times rand\left(n_{particles}, m_{dimensions}\right) \tag{12}$$

PSO attempts to improve the fitness function by decreasing the reciprocal knowledge I(y) between the components, as expressed in Equation (13):

$$I(y_i, y_j) = \sum_{i\neq j} p(y_i, y_j) \log\left(\frac{p(y_i, y_j)}{p(y_i)\, p(y_j)}\right) \sum_{i\neq j} p(Wx_i, Wx_j) \log\left(\frac{p(Wx_i, Wx_j)}{p(Wx_i)\, p(Wx_j)}\right) \tag{13}$$

If I (y_i, y_j) = 0, then y_i, y_j can be set independently and separately, and the fitness function defined as the following:

$$\text{Fit}(y) = I(y_i, y_j), \quad y_i,\ y_j \in y,\ i \neq j \tag{14}$$

Moreover, the maximization of entropy implies a higher level of independence between signals in respect of

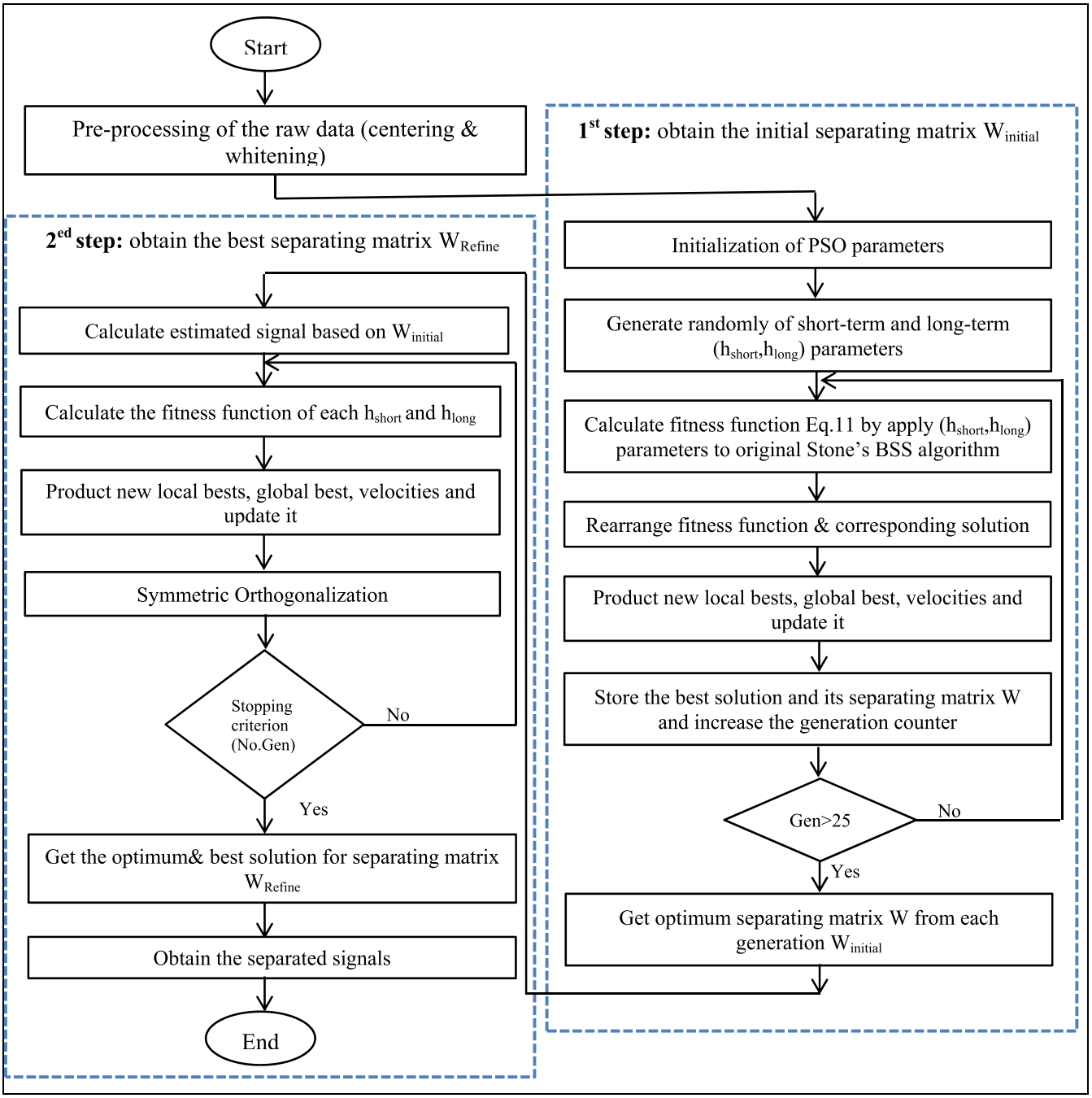

FIGURE 10. Flowchart of the proposed algorithm.

the principle of maximization of mixed-signal entropy because $I\left(y_i, y_j\right)$ is non-negative and, thus, $H\left(y_i\right) \geq H\left(y_1, y_2, \ldots, y_n\right)$. The optimal solution and distinct signals can be obtained with the rewriting Equation (9) in addition to the PSO algorithm:

$$\mathbf{y}\,(k) = \mathbf{W}_{\text{Refine}}\mathbf{x}\,(k) \tag{15}$$

Prior to each generation, symmetric orthogonalization is used to ensure independence amongst separate, applicable sources. The symmetric orthogonalization is obtained by [19]:

$$\mathrm{W} = \mathrm{W} \times \text{real}\left(\left(\mathrm{WW}^{\mathrm{T}}\right)^{-\frac{1}{2}}\right) \tag{16}$$

where w is the separating matrix which generated and tuned from PSO. The flow diagram of the suggested algorithm in Figure 10 is seen in a simple comparison. The last step after the EEG artefact removing is to recreate the EEG data, as illustrated by Figure 11. The reconstruction algorithm can be used to evaluate the temporal structure of $S(t)$ components

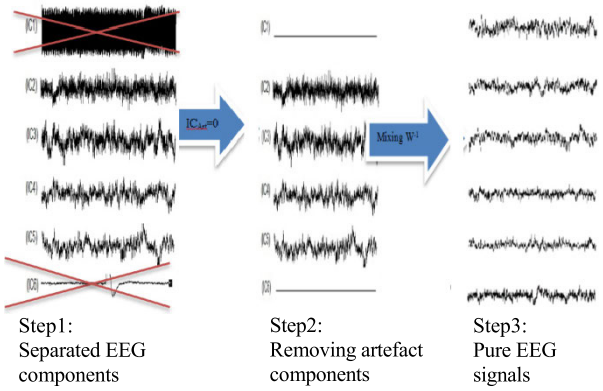

FIGURE 11. Reconstruction process based on the classical way.

and classify components of artefacts. On the standard basis, the artifact-specific components are set to zero, $S_{artf}(t) = 0$ (i.e., IC6 = 0), and the EEG-data are stated as follows:

$$\hat{x}(t) = A\,\hat{s}(t) \tag{17}$$

where $\hat{\mathbf{x}}(t)$ expresses the data free of the artefact, A is the fusing matrix $A = W^{-1}$, W is the non-mixing matrix and $\hat{S}(t)$ is a new component matrix. To check the rejection efficiency of electrooculogram (EOG) and power line artefacts, the separation process is calculated by the simulated data through the interference signal ratio (ISR) in [20]. However, in the real EEG data, the ISR calculation is not valid since no information on sources is available.

IV. RESULTS AND DISCUSSION

In order to check their performance, ISBSS is being compared with the original SBSS, EFICA, FastICA, and JADE. The current technique yields quite effective insulation in the real 9-channel data set of power line noise and EOG artefacts, where the power line noise interference is located and segregated in IC1 by the ISBSS algorithm; the EOG artefact is precisely isolated in IC6, as shown in Figure 12.

The mixture detection is based on the non-complex system of measurements described in the equation of the sparsity measure (17), as follows. [21]:

$$\text{Sparsity}\left(y^{(j)}\right) = \frac{\max\left[\left|y_i^{(j)}\right|\right]}{\text{std}\left[y_i^{(j)}\right]} \log\left(\frac{\text{std}\left[y_i^{(j)}\right]}{\text{median}\left[\left|y_i^{(j)}\right|\right]}\right) \tag{18}$$

where the j^{th} ingredient is $y^{(i)} = \left[y_1^{(j)}, \ldots, y_N^{(j)}\right]$, the sample size in the framework is N, the ideal perversion is std, and the period indicator is i. Very strong rejection is achieved by the proposed artefact algorithms, which display simple EOG artefact separation by IC6, and the power line noise interference located in IC1 (see Figure 12 and Table 1).

Figure 13 describes the correlation between both the artefact-reference signal and the extracted EOG artefact. The correlation result shows that the ISBSS approach is more

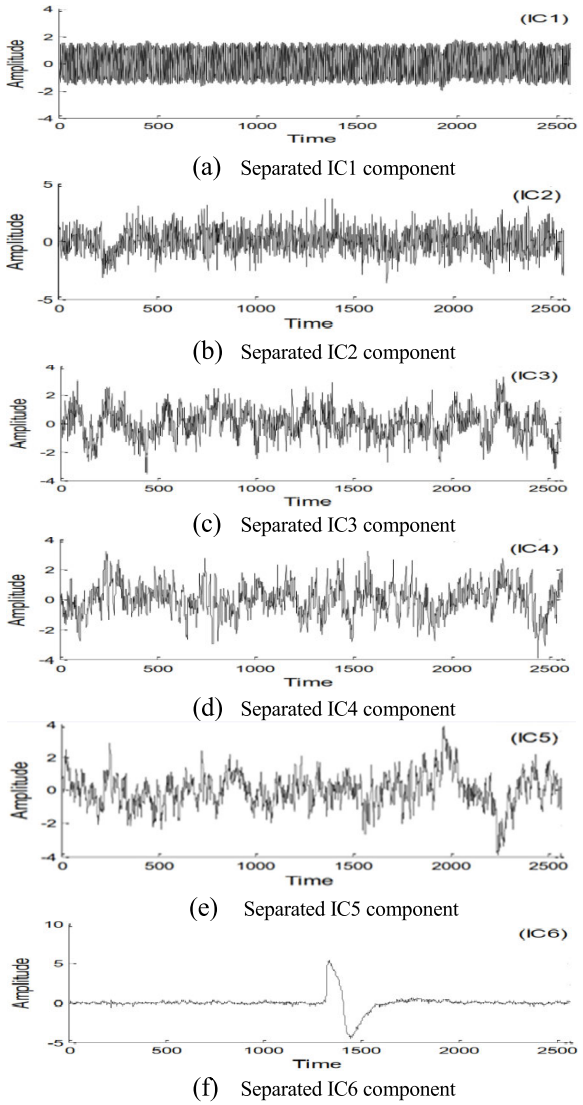

FIGURE 12. Separated signals of the real EEG 9-channel data set by ISBSS.

TABLE 1. Sparsity measure description of the separated signals.

IC	Sparsity	Type of IC
IC_1	0.1552	Line noise
IC_2	1.6597	Brain signal
IC_3	1.5930	Brain signal
IC_4	1.8253	Brain signal
IC_5	1.9646	Brain signal

effective than other BSS methods for eliminating the EOG artefact.

The power spectra of the mixed signals and the extracted components are shown in Figures 14 and 15. All channels, as described above, are 50-Hz power line noise intrusion, in particular O1, O2, C3, and C4.

We applied the proposed algorithms and various BSS algorithms to 19 channels of 10-second data to remove 50-Hz power line noise and EOG artefacts. Figure 16 shows the excluded components based on ISBSS. The power line

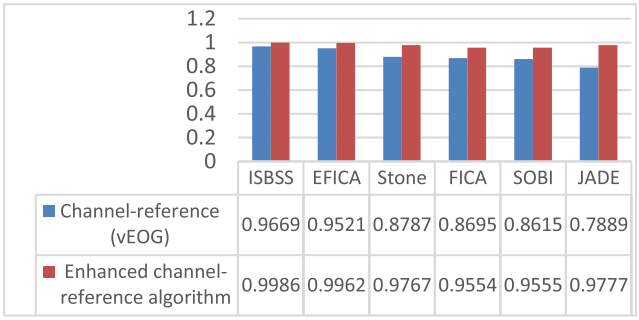

	ISBSS	EFICA	Stone	FICA	SOBI	JADE
Channel-reference (vEOG)	0.9669	0.9521	0.8787	0.8695	0.8615	0.7889
Enhanced channel-reference algorithm	0.9986	0.9962	0.9767	0.9554	0.9555	0.9777

FIGURE 13. The correlation between the artefact-reference signal and the EOG extracted artefact.

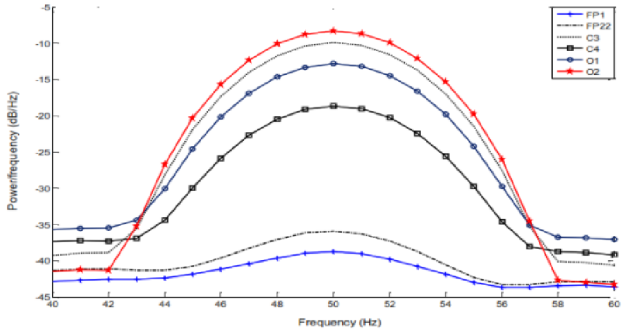

FIGURE 14. Frequency components of the recorded EEG (data set I) approximately 50 Hz.

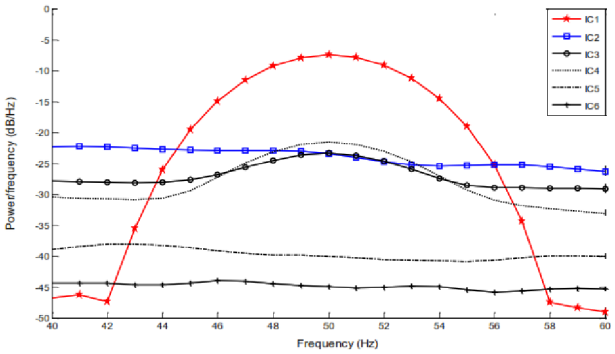

FIGURE 15. Frequency components of the ISBSS extracted components in 50 Hz.

noise interference was successfully separated in IC7 and the EOG artefact was isolated in IC1. The correlation measure between artefact-reference signal and the estimated artefacts (EOG, LN) component can test the performance of the proposed algorithms. The results obtained by the proposed algorithm (ISBSS) are better than those of the other BSS techniques, where the best correlation is obtained by ISBSS, and the JADE technique gets the worse value.

Figure 17 shows the signals of mixture 1 (EEG with LN-Figure 7) separated by the ISBSS algorithm. The collected signals are placed vertically for display purposes (on the top), and the corresponding recovered signal is on the bottom.

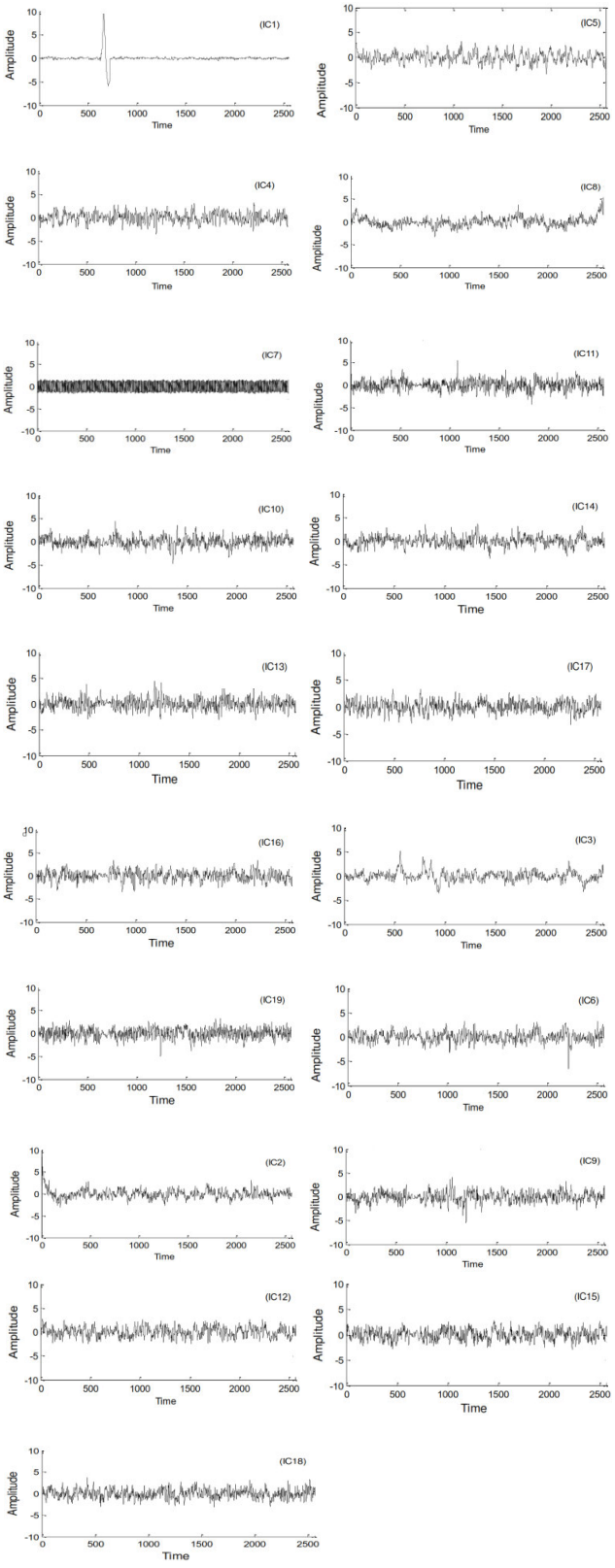

FIGURE 16. Separated signals by ISBSS algorithm.

Figure 18 shows the signals of mixture 2 (EEG with EOG- Figure 8) separated by the ISBSS algorithm; the processed signal is placed vertically for display purposes

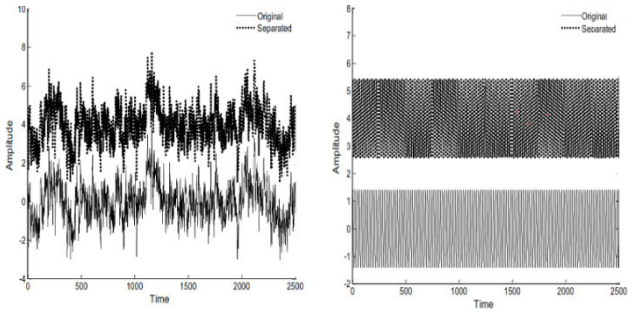

(A) EEG signal (B) LN

FIGURE 17. Original and separated signals by ISBSS for mixture 1.

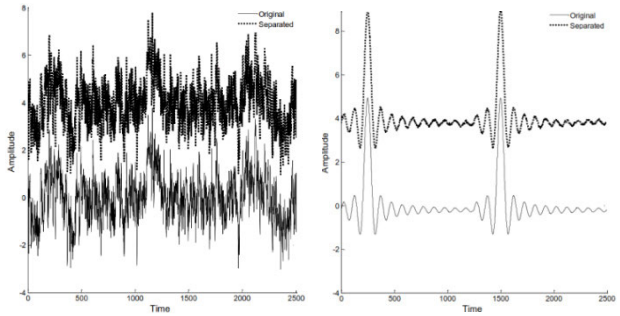

(A) EEG signal (B) EOG signal

FIGURE 18. Sources and separated signals by ISBSS for mixture 2.

(on the top), and the corresponding extracted signal is on the bottom.

Figure 19 shows the recovered signals of mixture 3 (EEG, LN, and EOG- Figure 9) by the ISBSS algorithm. The extracted signal is vertically shifted for show purposes (on the top), and the corresponding recovered signal is on the bottom.

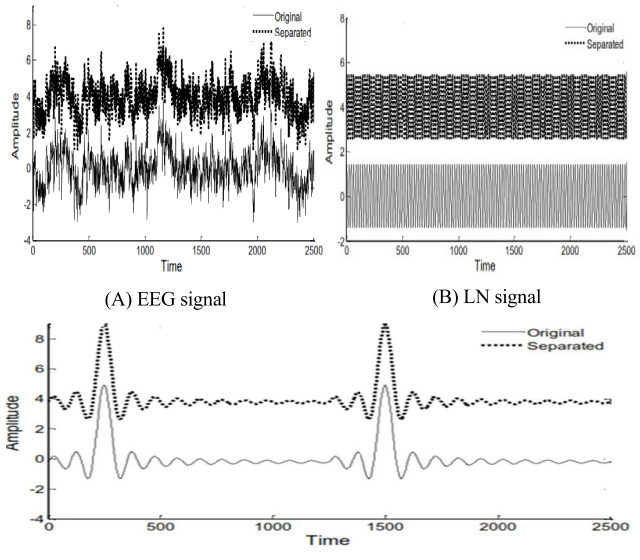

(A) EEG signal (B) LN signal

(C) EOG signal

FIGURE 19. Sources and separated signals by ISBSS for mixture 3.

Two indices are utilized to verify efficacy: the CIR and the integrated square error. CIR [20] uses equation (18) for estimating the execution of simulated results, where s(k) refers to the original signals, y(k) refers to the signals retrieved, and k to the time or sample index:

$$CIR_i = 10 \log \frac{E\left[\left(s_i\left(k\right) - y_i(k)\right)^2\right]}{E\left[\left(s_i(k)\right)^2\right]} \tag{19}$$

The success of the separating procedure is better when the CIR measure is small, as shown in Figure 20 to Figure 22. These figures show the comparison of CIR measures between different BSS algorithms. The average value of the performance indices for the proposed algorithm ISBSS is significantly surpassed for other BSS algorithms. Figure 20 shows the performance index compression for separating signals from mixture 1. The effects of the phase of separation are higher because of the reduction in CIR estimation. ISBSS (−60.5738 dB) displays the performance and the worst value is found by SOBI (−42.0495 dB).

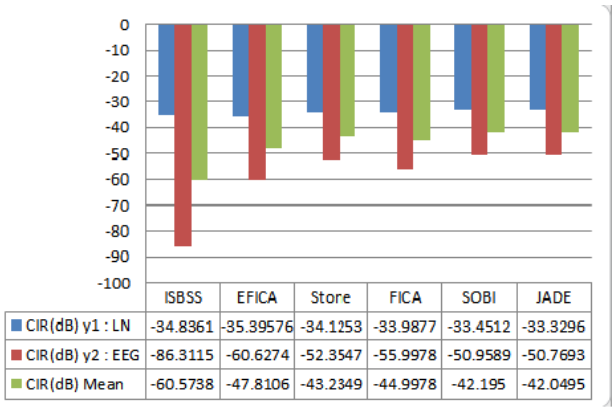

	ISBSS	EFICA	Store	FICA	SOBI	JADE
CIR(dB) y1 : LN	-34.8361	-35.39576	-34.1253	-33.9877	-33.4512	-33.3296
CIR(dB) y2 : EEG	-86.3115	-60.6274	-52.3547	-55.9978	-50.9589	-50.7693
CIR(dB) Mean	-60.5738	-47.8106	-43.2349	-44.9978	-42.195	-42.0495

FIGURE 20. The compression of the performance index for separating signals from mixture 1.

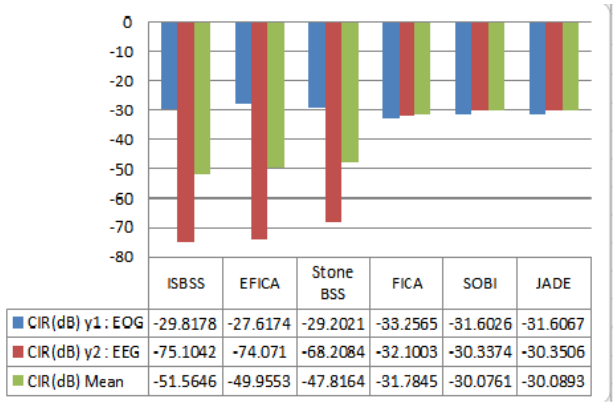

	ISBSS	EFICA	Stone BSS	FICA	SOBI	JADE
CIR(dB) y1 : EOG	-29.8178	-27.6174	-29.2021	-33.2565	-31.6026	-31.6067
CIR(dB) y2 : EEG	-75.1042	-74.071	-68.2084	-32.1003	-30.3374	-30.3506
CIR(dB) Mean	-51.5646	-49.9553	-47.8164	-31.7845	-30.0761	-30.0893

FIGURE 21. The compression of the performance index for separating signals from mixture 2.

An integral square error (ISE) is the second index that is used to track performance, as follows:

$$ISE = \sum_{K=0}^{T} \left(S_i\left(k\right) - y_i\left(k\right)\right)^2 \tag{20}$$

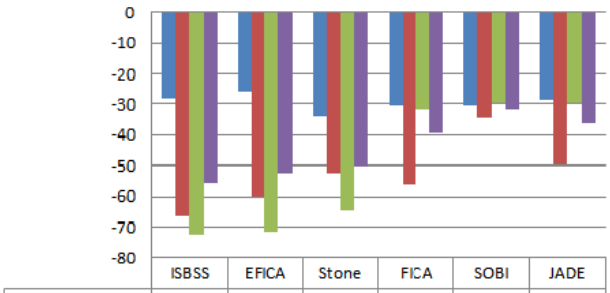

	ISBSS	EFICA	Stone	FICA	SOBI	JADE
CIR(dB) y1 : LN	-27.9257	-26.1559	-33.9812	-30.3523	-30.6898	-28.78
CIR(dB) y2 : EOG	-66.5205	-60.1094	-52.7812	-55.9096	-34.2503	-49.5674
CIR(dB) y3 : EEG	-72.5359	-71.5945	-64.4604	-31.3082	-29.4202	-29.4057
CIR(dB) Mean	-55.6607	-52.5199	-50.4076	-39.19	-31.4534	-35.9177

FIGURE 22. The compression of the performance index for separating signals from mixture 3.

The success of the separating procedure is better when the ISE measure is small, as shown in Figure 23 to Figure 25. These tables show the comparison of ISE measures between different BSS algorithms. The average value of the performance indices for the proposed algorithm is significantly surpassed for other BSS algorithms.

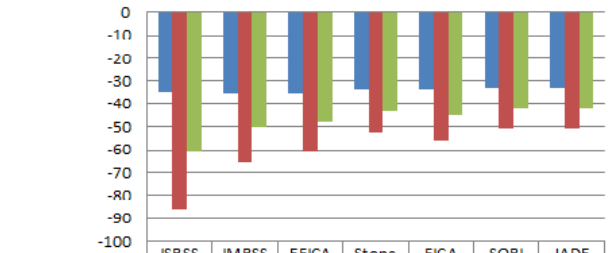

	ISBSS	IMBSS	EFICA	Stone	FICA	SOBI	JADE
ISE(dB) y1 : LN	34.8361	35.3358	35.3058	34.1253	33.9877	33.4512	33.3206
ISE(dB) y2 : EEG	-86.3115	-65.1643	-60.6274	-52.3547	-55.9978	-50.9589	-50.7693
ISE(dB) Mean	-60.5738	-50.2501	-47.8106	-43.2349	-44.9978	-42.195	-42.0495

FIGURE 23. Performance index compression for separating signals from mixture 1.

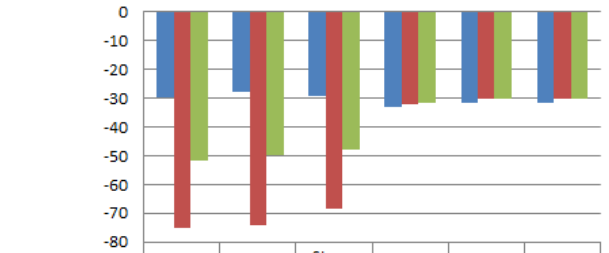

	ISBSS	EFICA	Stone BSS	FICA	SOBI	JADE
ISE(dB) y1 : EOG	-29.8178	-27.6174	-29.2021	-33.2565	-31.6026	-31.6067
ISE(dB) y2 : EEG	-75.1042	-74.071	-68.2084	-32.1003	-30.3374	-30.3506
ISE(dB) Mean	-51.5646	-49.9553	-47.8164	-31.7845	-30.0761	-30.0893

FIGURE 24. Performance index compression for separating signals from mixture 2.

Figure 25 shows the integral square error (ISE), value for the EEG, EOG, and LN signal, as well as three well-known BSS algorithms (JADE, EFICA, SOBI) and two Stone's BSS algorithms (Stone BSS, ESBSS), of which ESBSS refers to the evolutionary Stone's BSS algorithm as presented by in [22], which is based on a hybridization of Stone's BSS and metaheuristic algorithm called genetic algorithm for electroencephalogram (EEG) artefact extraction.

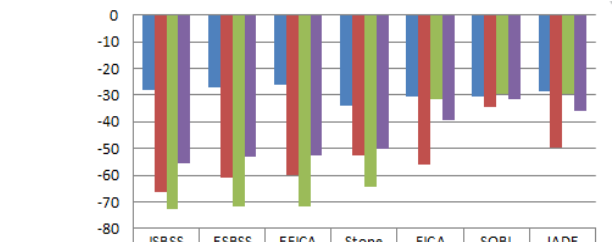

	ISBSS	ESBSS	EFICA	Stone	FICA	SOBI	JADE
ISR(dB) y1 : LN	-27.9257	-26.9989	-26.1559	-33.9812	-30.3523	-30.6898	-28.78
ISR(dB) y2 : EOG	-66.5205	-60.9954	-60.1094	-52.7812	-55.9096	-34.2503	-49.5674
ISR(dB) y3 : EEG	-72.5359	-71.9842	-71.5945	-64.4604	-31.3082	-29.4202	-29.4057
ISR(dB) Mean	-55.6607	-53.3262	-52.6199	-50.4076	-39.19	-31.4534	-35.9177

FIGURE 25. Performance ISE index compression for separating signals from mixture 3.

Table 2 displays the spectral density estimation (SDE) value for the raw EEG signal to determine the effectiveness, as well as two single-channel techniques for EOG extraction and removal such as (ECR) and (SG), of which ECR refers to the Enhanced Channel-Reference algorithm, is discussed and presented by Zhu and Abdullah [23], and SG refers to the Savitzky-Golay algorithm which is discussed and presented by Szibbo *et al.* [8].

TABLE 2. Spectral density estimation (SDE).

Algorithm	SDE Value
EEG (raw)	38.1411
ECR	3.5253
SG	2.1637
ISBSS	1.0114

Welch's method used to determine the SDE value in the suggested system, which is less than that of other algorithms.

V. CONCLUSION

In this study, present a new application for Stone's Blind Source Separation method in brain signal analysis to separate an Electrooculogram (EOG) and Power Line Noise Artefacts from Electroencephalogram (EEG) Mixtures with PSO hybridization to enhance the separation process.

The proposed algorithm is shown to be an efficient technique for extracting EOG and LN artefacts from EEG brain mixtures compared to other algorithms, such as the original SBSS, EFICA, SOBI, and JADE. The performance of the ISBSS is better than the various types of BSS algorithms, as shown in the simulated and real EEG data.

The efficacy assessment proves that Stone's BSS algorithm is a valuable medical technique to distinguish various artefact forms from EEG information. In this study, ISBSS was demonstrated to reject and remove electrooculogram (EOG) and power line noise artefacts from electroencephalogram (EEG) mixtures.

Other artefacts such as ballistocardiogram (BCG) and electromyogram (EMG) artefacts can occur in EEG signals for future work. ISBSS should be a valuable algorithm to reject these artefacts. This research can now be expanded to reject new kinds of artefacts, such as BCG and EMG and can be expanded with a further machine learning algorithm or soft computing techniques to hybridize Stone's BSS, such as artificial bee colony algorithms (BCA), and the runner-root algorithm (RRA).

To check the effectiveness and feasibility of this method when the EEG signals have changes need to apply in real-time application.

Recently, the world directed toward wireless EEG instead of wire EEG system for easy and more flexible in different applications particularly for Brain-computer interface system BCI, but the measured EEG signals are subject to heavy motion and vibration artefacts. The conventional methods to separate these artefacts unsuccessful, therefore we recommended using blind source separation techniques for artefact extraction and then removing. Wireless EEG systems eliminate the wire connection between the signal acquisition and the translation part, with a wireless transmission unit such as Bluetooth.

DATA AVAILABILITY

The data used to validate the results are accessible on request from the author.

ACKNOWLEDGMENT

The research is sponsored by the South China University of Technology International Exchange Program. The authors thank Dr. Ali Al-Jaradi, Al-Jomhori hospital, Taiz, Yemen, and Dr Ahmed Kareem Abdullah, Foundation of Technical Education, Al-Musaib Technical College, Babel, Iraq, for their efforts for giving them real data (19 channels).

CONFLICTS OF INTEREST

There are no conflicts of interest concerning the publishing of this article.

REFERENCES

[1] S. Mortaheb, F. Rostami, S. Shahin, and R. Amirfattahi, "Wavelet-based single-trial event-related potential extraction in very low SNR conditions," in *Proc. 6th Int. Conf. Comput. Knowl. Eng. (ICCKE)*, 2016, pp. 82–87, doi: 10.1109/ICCKE.2016.7802120.

[2] F. L. Chang, S. Nam, and A. Nijholt, *Brain-Computer Interfaces Handbook: Technological and Theoretical Advances*. 2018.

[3] *Signal Processing and Machine Learning for Brain-Machine Interfaces*, Inst. Eng. Technol., London, U.K., 2018.

[4] C. Corradino, S. Member, and M. Bucolo, "Automatic preprocessing of EEG signals in long time scale," in *Proc. 37th Annu. Int. Conf. IEEE Eng. Med. Biol. Soc. (EMBC)*, Aug. 2015, pp. 4110–4113.

[5] H. Gauba, P. Kumar, P. Pratim, P. Singh, D. Prosad, and B. Raman, "Prediction of advertisement preference by fusing EEG response and sentiment analysis," *Neural Netw.*, vol. 92, pp. 1–12, Aug. 2017, doi: 10.1016/j.neunet.2017.01.013.

[6] X. Chen, A. Liu, Q. Chen, Y. Liu, L. Zou, and M. J. McKeown, "Simultaneous ocular and muscle artifact removal from EEG data by exploiting diverse statistics," *Comput. Biol. Med.*, vol. 88, pp. 1–10, Sep. 2017, doi: 10.1016/j.compbiomed.2017.06.013.

[7] N. Mammone, F. La Foresta, and F. C. Morabito, "Automatic artifact rejection from multichannel scalp EEG by wavelet ICA," *IEEE Sensors J.*, vol. 12, no. 3, pp. 533–542, Mar. 2012, doi: 10.1109/JSEN.2011.2115236.

[8] D. Szibbo, A. Luo, and T. J. Sullivan, "Removal of blink artifacts in single channel EEG," in *Proc. Annu. Int. Conf. IEEE Eng. Med. Biol. Soc.*, Aug. 2012, pp. 3511–3514, doi: 10.1109/EMBC.2012.6346723.

[9] A. Gonzalez, I. Nambu, H. Hokari, and Y. Wada, "EEG channel selection using particle swarm optimization for the classification of auditory event-related potentials," *Sci. World J.*, vol. 2014, pp. 1–11, Mar. 2014, doi: 10.1155/2014/350270.

[10] S. S. Priyadharsini and S. E. Rajan, "Performance analysis of swarm intelligence algorithms in removal of ECG artefact from tainted EEG signal," *Automatika*, vol. 59, nos. 3–4, pp. 408–415, Oct. 2018, doi: 10.1080/00051144.2018.1541642.

[11] C. Kaur and P. Singh, "EEG artefact suppression based on SOBI based ICA using wavelet thresholding," in *Proc. 2nd Int. Conf. Recent Adv. Eng. Comput. Sci. (RAECS)*, Dec. 2015, pp. 13–16, doi: 10.1109/RAECS.2015.7453319.

[12] A. K. Abdullah and C. Z. Zhang, "Enhancement of source separation based on efficient stone's BSS algorithm," *Int. J. Signal Process., Image Process. Pattern Recognit.*, vol. 7, no. 2, pp. 431–442, Apr. 2014.

[13] M. A. Ahmed, Q. Deyu, and E. N. Alshemmary, "Electroencephalogram signal eye blink rejection improvement based on the hybrid stone blind origin separation and particle swarm optimization technique," *IEEE Access*, vol. 8, pp. 105671–105680, 2020, doi: 10.1109/ACCESS.2020.2999562.

[14] G. Grimaldi, M. Manto, and Y. Jdaoudi, "Quality parameters for a multimodal EEG/EMG/kinematic brain-computer interface (BCI) aiming to suppress neurological tremor in upper limbs," *FResearch*, vol. 2, p. 282, Dec. 2013, doi: 10.12688/f1000research.2-282.v1.

[15] B. Singh and H. Wagatsuma, "A removal of eye movement and blink artifacts from EEG data using morphological component analysis," *Comput. Math. Methods Med.*, vol. 2017, pp. 1–17, Jan. 2017, doi: 10.1155/2017/1861645.

[16] G. Ouyang, A. Hildebrandt, F. Schmitz, and C. S. Herrmann, "Decomposing alpha and 1/f brain activities reveals their differential associations with cognitive processing speed," *NeuroImage*, vol. 205, Jan. 2020, Art. no. 116304, doi: 10.1016/j.neuroimage.2019.116304.

[17] T. Rasheed, "Constrained blind source separation of human brain signals constrained blind source separation of human brain signals," Kyung Hee Univ., Seoul, South Korea, Tech. Rep., 2010.

[18] V. Krishnaveni, S. Jayaraman, P. M. M. Kumar, K. Shivakumar, and K. Ramadoss, "Comparison of independent component analysis algorithms for removal of ocular artifacts from electroencephalogram," *Science*, vol. 5, Aug. 2005.

[19] S. Mavaddaty and A. Ebrahimzadeh, "Blind signals separation with genetic algorithm and particle swarm optimization based on mutual information," *Radioelectron. Commun. Syst.*, vol. 54, no. 6, pp. 315–324, Jun. 2011, doi: 10.3103/S0735272711060045.

[20] M. F. Issa and Z. Juhasz, "Improved EOG artifact removal using wavelet enhanced independent component analysis," *Brain Sci.*, vol. 9, no. 12, p. 355, Dec. 2019.

[21] S. K. Goh, H. A. Abbass, K. C. Tan, A. Al-Mamun, C. Wang, and C. Guan, "Automatic EEG artifact removal techniques by detecting influential independent components," *IEEE Trans. Emerg. Topics Comput. Intell.*, vol. 1, no. 4, pp. 270–279, Aug. 2017, doi: 10.1109/TETCI.2017.2690913.

[22] A. K. Abdullah, C. Z. Zhang, A. A. A. Abdullah, and S. Lian, "Automatic extraction system for common artifacts in EEG signals based on evolutionary stone's BSS algorithm," *Math. Problems Eng.*, vol. 2014, pp. 1–25, Aug. 2014, doi: 10.1155/2014/324750.

[23] C. Z. Zhang and A. K. Abdullah, "Discussion of approach for extracting pure EOG reference signal from EEG mixture based on wavelet denoising technique," *J. Biomimetics, Biomater. Biomed. Eng.*, vol. 23, pp. 9–17, Jun. 2015, doi: 10.4028/www.scientific.net/JBBBE.23.9.

MOHAMMED ALI AHMED received the M.Sc. degree in computer science from Harbin Engineering University, Harbin, China. He has programming experience and technological research experience in machine learning. His research interests include machine learning algorithms and software, feature selection, and biomedical, big data, information retrieval, and bioinformatics learning.

DEYU QI received the Ph.D. degree. He is currently a Professor of engineering, a Ph.D. Supervisor, and the Director of the Institute of Computer Systems, South China University of Technology. His main research interests include software development methods, system structure, intelligent control, and so on.

EBTESAM N. ALSHEMMARY received the M.Sc. and Ph.D. degrees from the University of Technology, Baghdad, in 1999 and 2007, respectively. She was a Rapporteur with the Computer Department, Faculty of Education for Girls, University of Kufa, Iraq, where she is currently an IT-RDC Manager. Her specializations are computer and control engineering and mechatronics engineering (robotics and image processing). She is especially well-known for profound contributions to different fields of computer programs, biometrics, and automatic identification systems. She has published research in international and local journal in computer science. Her research interests include statistical analyses of health, medical studies, and information technology. She was a member of many committees with the University of Kufa, such as scientific and examination committees. She is a member of the Editorial and the Reviewer Board of the *International Journal of Electronics and Computer Science Engineering (IJECSE)*. She is also a member of the Reviewer Board of *European Journal of Science and Engineering (EJSE)*, a Reviewer of *IET Image Processing* Journal, and the Editorial Board of the *International Journal of Advanced Computer Science and Information Technology (IJACSIT)*.